# 7-Ketocholesterol Is Present in Lipid Deposits in the Primate Retina: Potential Implication in the Induction of VEGF and CNV Formation

*Ernesto F. Moreira, Ignacio M. Larrayoz, Jung Wha Lee, and Ignacio R. Rodríguez*

**Purpose.** 7-Ketocholesterol is a highly toxic oxysterol found in abundance in atherosclerotic plaques and is believed to play a critical role in atherosclerosis. The purpose of this study was to identify and localize 7-ketocholesterol (7kCh) in the primate retina and to examine the potential consequences of its presence in oxidized lipid deposits in the retina.

**Methods.** Unsterified 7kCh was identified and quantified by high-performance liquid chromatography-mass spectrometry. Localization of 7kCh was performed by immunohistochemistry. VEGF induction was determined by qRT-PCR. Cell viability was determined by measuring cellular dehydrogenase activity. Analyses were performed using ARPE19 and human vascular endothelial cells (HMVECs).

**Results.** 7-Ketocholesterol is localized mainly to deposits in the choriocapillaris and Bruch's membrane and on the surfaces of vascular endothelial cells of the neural retina. RPE/choriocapillaris regions contained approximately four times more 7kCh than the neural retina. In ARPE19 cells and HMVECs, oxidized LDL and 7kCh induced VEGF 8- to 10-fold above controls. Hypoxia inducible factor (HIF)-1$\alpha$ levels did not increase as a result of 7kCh treatment, suggesting an HIF-independent induction pathway. Cholesterol sulfate, a liver X receptor (LXR) antagonist, had marked attenuation of the 7kCh-mediated VEGF induction. LXR-specific siRNAs also reduced VEGF induction. Inhibition of NF-$\kappa$B with BAY 11-7082 reduced IL-8 but not VEGF induction.

**Conclusions.** The location of 7-kCh in the retina and its induction of VEGF in cultured RPE cells and HMVECs suggest it may play a critical role in choroidal neovascularization. The pathway for VEGF induction seems to be independent of HIF-1$\alpha$ and NF-$\kappa$B but seems to be partially regulated by LXRs. (*Invest Ophthalmol Vis Sci.* 2009;50:523–532) DOI:10.1167/iovs.08-2373

Seven-ketocholesterol (7kCh) is a toxic cholesterol oxide found in high levels in atherosclerotic plaques[1] and is suspected of being involved in foam cell formation in macrophages.[2,3] In vivo, cholesterol and cholesteryl esters found in LDL deposits form 7kCh through the Fenton reaction.[4] This oxidation is usually catalyzed by copper and iron ions,[5] which are relatively abundant in atherosclerotic plaques.[6] Cholesteryl esters (CEs) are particularly susceptible to copper oxidation,[4,5] making the CE-rich LDL-derived deposits commonly found in capillaries and arteries highly susceptible to this form of oxidation. Another path for the formation of 7kCh is photooxidation, which has been well described in vitro[7] and may play an important role in the skin and retina. Cholesterol can be readily photooxidized in the presence of a suitable photosensitizer to form a series of hydroperoxide intermediates[8,9] that can further oxidize to 7kCh. Both pathways may be sources of 7kCh in the retina.

Vascular endothelial growth factor (VEGF) is a member of a family of cytokines best known for its role in promoting angiogenesis, maintaining vascular permeability, promoting hematopoietic cell development, and wound healing.[10] VEGF expression is known to be affected by hypoxia[11] and inflammation-related events.[12] The transcriptional regulation of VEGF is complex, and two key transcription factors are known to be involved in its regulation, hypoxia inducible factor (HIF)-1$\alpha$ and Sp1.[13] VEGF is also known to be induced by oxidized low-density lipoprotein (oxLDL)[14] and 7kCh.[15]

Hypoxia induces VEGF (and many other genes) through HIF-1$\alpha$. HIF-1$\alpha$ is a tightly regulated transcription factor[11] that, under normoxic conditions, is continuously synthesized and degraded.[11,16] Under hypoxic conditions HIF-1$\alpha$ degradation is inhibited, which allows it to travel to the nucleus and to dimerize with its partner, HIF-1$\beta$, to induce transcription.[16] A number of proteins and small molecules are known to regulate HIF-1 activity mainly by interacting with proteins involved in its degradation pathway.[16] Reactive oxygen species (ROS) are also known to play an important role in the induction of HIF-1$\alpha$ through a mitochondria-mediated process.[16,17]

VEGF is also known to be induced via HIF-independent pathways,[12] which may be related to hypoxia and/or inflammation depending on the circumstances. These are the Ras oncogene,[18] the nuclear factor $\kappa$B (NF-$\kappa$B),[19,20] and the liver X receptors (LXRs)-mediated pathways.[21] Ras involvement was first demonstrated in HIF-1$\alpha^{-/-}$ mice when "tumors" generated with K-RAS-transformed embryonic fibroblast cells maintained their angiogenesis.[18] This suggested that K-RAS could compensate for the loss of HIF function and maintain VEGF induction. Additional studies have shown the involvement of the Ras pathways in VEGF induction.[12] NF-$\kappa$B is an important transcription factor that mediates hypoxic and inflammatory responses and has been shown to be pivotal in the induction of VEGF.[19,20] The NF-$\kappa$B activation of VEGF may be dependent on K-RAS or mitochondrial reactive oxygen species (ROS).[12]

The LXR pathway for the induction of VEGF is particularly interesting because oxysterols such as 7kCh are agonistic ligands for LXRs.[22] Although 7kCh is not a particularly potent agonist for LXR,[23] it may be able to induce VEGF if it accumulates in sufficient amounts.

In this study we demonstrate that 7kCh is present in the primate retina and is localized mainly to Bruch's membrane and the choriocapillaris associated with suspected lipoprotein deposits. We also demonstrate that 7kCh can induce VEGF

From the Section on Mechanisms of Retinal Diseases, National Eye Institute, National Institutes of Health, Bethesda, Maryland.

Supported by the National Eye Institute Intramural Research Program.

Submitted for publication June 3, 2008; revised July 29 and September 5, 2008; accepted December 9, 2008.

Disclosure: **E.F. Moreira**, None; **I.M. Larrayoz**, None; **J.W. Lee**, None; **I.R. Rodríguez**, None

The publication costs of this article were defrayed in part by page charge payment. This article must therefore be marked "*advertisement*" in accordance with 18 U.S.C. §1734 solely to indicate this fact.

Corresponding author: Ignacio R. Rodríguez, National Eye Institute, National Institutes of Health, Section on Mechanisms of Retinal Diseases, LRCMB, 7 Memorial Drive, MSC0706, Building 7, Room 302, Bethesda, MD 20892; rodriguezi@nei.nih.gov.

expression in cultured RPE cells and vascular endothelial cells. More important, we demonstrate that 7kCh-mediated VEGF induction is HIF-1$\alpha$ independent and is partially regulated by LXRs.

## Materials and Methods

### Materials

Cholesterol (Ch) and 7kCh were purchased from Steraloids, Inc. (Newport, RI). For high-performance liquid chromatography-mass spectroscopy (HPLC-MS), acetonitrile and methanol Optima grade were purchased from Fisher Scientific (Fair Lawn, NJ). High-purity water was purchased from Fisher Scientific and was used for ultraviolet light and mass spectroscopy. Hydroxypropyl-$\beta$-cyclodextrin (HPBCD) and $CoCl_2$ were purchased from Sigma-Aldrich (St. Louis, MO). LXR antagonists cholesterol-3-sulfate (ChS) and 7kCh-3-sulfate (7kChS) were synthesized as previously described[24] and were purified by HPLC. Their authenticity was verified by LC-MS. The mouse monoclonal antibody specific for 7kCh (anti-7kCh) was obtained from the Japanese Institute for the Control of Aging (Shizuoka, Japan) and was used as previously described.[25] Mouse anti–human HIF-1$\alpha$ antibody was purchased from BD Biosciences (San Jose, CA).

### Preparation of LDL

LDL was purified from human serum by ultracentrifugation, as previously described.[26] Copper-oxidized LDL and LDL containing approximately 15% 7kCh (7kLDL) were prepared as previously described.[4,27]

### Extractions of Lipids from Retina

Retinal tissues were dissected, and the lipids were extracted as previously described.[28] The lipids were then dissolved in methanol and analyzed directly. Samples were not saponified to prevent breakdown of 7kCh during the alkaline hydrolysis. Thus, this protocol detects only the free sterols and may underestimate the total levels of 7kCh.

### High-Pressure Liquid Chromatography and Mass Spectroscopic Detection of 7kCh

HPLC was performed (model 2695; Waters, Milford, MA) with a photo diode array detector (2996 PDA; Waters) and a mass spectrometer (QTOF-Micro; Waters) using atmospheric pressure chemical ionization (APCi). Chromatography conditions were similar to those previously described.[29] The column (2.1 mm × 250 mm, XTerra RP18; Waters) was run at 0.2 mL/min. The initial mobile phase consisted of water/acetonitrile (4:1, vol/vol) containing 0.1% formic acid. Chromatography was performed with two linear gradients. The first gradient increased the acetonitrile from 20% to 100% in 15 minutes and held at 100% for 5 minutes. The second gradient started at 20 minutes from 100% acetonitrile to 100% methanol for 15 minutes and was maintained for 3 minutes before re-equilibration to the initial water/acetonitrile mixture. The entire solvent flow (0.2 mL/min) was diverted to the APCi probe. APCi ionization was performed (IonSABRE APCi; Waters) with the probe temperature set at 500°C and the source temperature at 120°C. At the source, the corona was set at 10 $\mu$A, the sample cone was set at 20 V, and the extraction cone was set at 3 V. Cone gas flow was set at 50 L/h, and the dissolvation gas flow was set at 600 L/h. Collision energy in the quadrupole was set to 7 V for MS and at 27 V for MS/MS, and 7kCh was quantified by integrating the total ion current (TIC) for the 401 m/z ion (M+H). Cholesterol was quantified using the TIC for the 369 m/z ion (M-OH). Amounts were reported as picomoles of 7kCh per nanomole of cholesterol after normalization to the internal standard $\beta$-sitosterol (m/z 397).

### Preparation of 7kCh Solutions in HPBCD

HPBCD-7kCh solutions were prepared as previously described.[30] 7kCh was weighed and wetted with dichloromethane and then was dissolved in the smallest volume possible of 100% ethanol. HPBCD (45% wt/vol) was dissolved in PBS and added to the 7kCh-ethanol solution in a glass graduated cylinder. The 45% HPBCD was added to the final volume required for 10 mM 7kCh solution. The solution was vigorously mixed and put into a 42°C oven to allow the ethanol and any lingering dichloromethane to evaporate. The HPBCD-7kCh solution was then adjusted to a final volume using distilled water. The 10 mM 7kCh solution was diluted to 1 mM using PBS, and this solution was added to the cells directly. The final concentration of HPBCD in cells receiving 10 $\mu$M 7kCh is 0.045%. ARPE19 cells and human vascular endothelial cells (HMVECs) tolerate HPBCD concentrations greater than 1% without any toxicity.

### Monkey Tissue Collection and Processing

All animal research was conducted in adherence to the ARVO Statement for the Use of Animals in Ophthalmic and Vision Research and in accordance with National Institutes of Health (NIH) guidelines for the care and use of animal in research. Monkey eyes were provided by the Pathology Department of the Division of Veterinary Resources after completion of approved institute protocols at the NIH. Fresh monkey eyes were collected immediately after euthanatization and were immersed in ice-cold, freshly prepared 4% formaldehyde (Polysciences, Warrington, PA) in 1× PBS after penetrating slits were made at the limbus. Eyes were left in the chilled fixative for 8 hours and were washed three times in 1× PBS (Biosource, Rockville, MD). Cryoprotection was performed by increasing concentrations of sucrose (5%–25%, wt/vol) in 0.1 M phosphate buffer (pH 7.4) after removal of the anterior segment and lens. Eyecups were cut into smaller pieces for convenience before flash freezing in a 2:1 (vol/vol) mixture of 25% buffered sucrose and OCT compound (Tissue-Tek; Ted Pella, Redding, CA). Ten-micrometer-thick sections were cut with a cryostat (CM3050 S; Leica, Wetzlar, Germany) and were stored at −20°C until ready for use.

### Immunohistochemistry

Monkey retinal sections (10 $\mu$m) were dried at room temperature (RT) for 30 minutes, and a hydrophobic circle was drawn around the specimen (Pap-pen; Polysciences). Endogenous peroxidase was inactivated in 3% $H_2O_2$ in PBS for 25 minutes. Sections were then blocked in ICC buffer containing 10% (vol/vol) normal goat serum (KPL, Gaithersburg, MD), 0.5% BSA, 0.2% Tween-20, and 0.05% sodium azide for 1 hour at 4°C. Sections were then incubated with mouse anti-7kCh antibody (at 1:100 dilution) overnight at 4°C. After they were washed with PBS, the sections were incubated with an anti-mouse biotinylated secondary antibody (Jackson ImmunoResearch Laboratories, West Grove, PA) for 1 hour at RT (1:200 dilution). Sections were washed again with PBS and incubated with the use of a peroxidase kit (Vectastain ABC; Vector Laboratories, Burlingame, CA) for 45 minutes at RT. The sections were developed using a peroxidase substrate kit (AEC; Vector Laboratories) according to the manufacturer's instructions. Reaction was stopped by several washes in PBS, and the sections were mounted on glass microscope slides (Aquamount; Polysciences). Image acquisition was performed using a Zeiss photomicroscope (Axioimage M1; Carl Zeiss MicroImaging, Thornwood, NY).

### Cell Cultures

ARPE19 cells were obtained from the ATCC (Manassas, VA) and were cultured as previously described.[27] HMVECs, a kind gift from Rong Shao (Pioneer Valley Life Sciences Institute, Springville, MA), were cultured and maintained as previously described.[31]

### cDNA Synthesis and Real-Time Quantitative RT-PCR

RNA extraction and cDNA synthesis were performed using Invitrogen (Carlsbad, CA) reagents and kits. All qRT-PCR experiments were performed three times. All TaqMan gene expression assays were performed in triplicate using ready-to-use probe and primer sets in an ABI

instrument (ABI 7500; Applied Biosystems, Foster City, CA) according to the manufacturer's specifications. For each cDNA, GAPDH (ABI 4352934E) was used as an endogenous standard to estimate the mRNA levels. VEGF-$\alpha$ (Hs00173626_m1), ABCA1 (Hs00194045_m1), IL-8 (Hs00174103_ml), and LXRs (LXR$\alpha$ [NR1H3], catalog number HS00172585_m1; LXR$\beta$ [NR1H2], catalog number HS01027215_g1) were measured relative to GAPDH. Results were normalized and expressed relative to standard controls and are shown as the average value; error bars are the SD from the mean (Figs. 3, 4, 5, 6, and 9).

### Cell Viability Assays

Cell viability assays were performed on a 24-well plate, and each measurement was performed in quadruplicate. Cell viability was measured with a cell counting kit (Cell Counting Kit-8; Dojindo Molecular Technologies, Gaithersburg, MD) that measures cellular dehydrogenase (mostly mitochondrial) activity.

### Immunoblot

Cells in 24-well plates were treated with increasing concentrations of 7kCh (5, 10, and 15 $\mu$M) or 100 and 200 $\mu$M $CoCl_2$. After 24 hours, cells were extracted in lysis buffer (MPER Solution; Pierce, Woburn, MA) in the presence of protease inhibitors (Roche, Indianapolis, IN). Protein was spun briefly to remove the nuclear fraction, and the supernatant was precipitated in 10% trichloroacetic acid. Samples (20 $\mu$g protein) were separated in a 4% to 12% Bis-Tris gel, transferred to a nitrocellulose membrane (Invitrogen, Carlsbad, CA) and probed with primary antibody against HIF-1a (1:500) at 4°C. The blot was developed using horseradish peroxidase-conjugated secondary antibody (1:2000; Pierce, Woburn, MA) and a chemiluminescent substrate (Supersignal West Pico Chemiluminescent Substrate; Pierce).

### Inhibition of LXRs with Cholesterol Sulfate

Treatment of ARPE19 cells with ChS and 7kChS was performed as previously described.[32] In brief, ARPE19 cells were seeded onto 24-well plates ($2.5 \times 10^5$ cells/well) and allowed to grow overnight. For ChS, cells were treated in serum-free media with 0 and 15 $\mu$M 7kCh with or without 20 $\mu$M ChS. qRT-PCR analyses were performed 24 hours after treatment.

### Electroporation and siRNA Knockdown of LXRs

Transfection of siRNA was performed by electroporation using an Amaxa instrument (Nucleofector II; Amaxa Biosystems, Gaithersburg, MD), as specified by the manufacturer. Two million ARPE19 cells were mixed with 2.5 $\mu$g siRNAs and 100 $\mu$L solution (Nucleofector V; Amaxa) and were electroporated according to the manufacturer's instructions. Cells were allowed to recover for 24 hours before treatment with 15 $\mu$M 7kCh. RNA for qRT-PCR was prepared 24 hours after oxysterol treatment. siRNAs were chosen from genome-wide siRNAs (HP OnGuard siRNA Design; Qiagen, Gaithersburg, MD), LXR$\beta$ (1 and 2, NR1H2; catalog numbers SI00094787 and SI00094801, respectively), LXR$\alpha$ (2 and 4, NR1H3; catalog numbers SI00080409 and SI00080430, respectively), and a nonspecific siRNA (AllStars negative control, catalog number 1027283) was used as a negative control.

### ELISA Assay for VEGF

VEGF levels in conditioned media from ARPE19 cells were determined 48 hours after treatment with 0, 4, 8, 12, 16, and 20 $\mu$M 7kCh using the human VEGF ELISA kit as specified by the manufacturer (Quantikinine; R&D Systems, Minneapolis, MN).

### Treatment of ARPE19 Cells with BAY-11-7082 NF-$\kappa$B Inhibitor

ARPE19 cells were treated with 1 and 2 $\mu$M BAY-11-7082 with and without 15 $\mu$M 7kCh. After 24 hours, the cells were collected for mRNA extraction and qRT-PCR as described.

## Results

### Identification and Quantification of 7kCh in Monkey Retina

Lipid extracts from monkey retina were analyzed by LC-MS, as described in Materials and Methods. Under these chromatography conditions, 7kCh has a retention time of 26.4 minutes. With the use of APCi, 7kCh formed a prominent m/z 401 ion (M+H) unique to 7kCh and some of its hydroperoxide intermediates. Results from the LC-MS analysis of one retina of a 7-year-old female rhesus monkey are shown in Figure 1. Total ion current for the 7kCh m/z 401 ion (M+H) is shown in Figure 1A, and the MS spectra for the 26.4-minute peak are shown in Figure 1B. Results clearly demonstrated that the neural retina (NR) and the pigment epithelium and choriocapillaris (PEC) fractions had detectable levels of 7kCh. The analysis in Figure 1 is representative of extracts from different monkeys and from human postmortem retina samples (data not shown). Quantification was performed by MS and normalized to free cholesterol. Amounts of 7kCh in the NR fractions of monkeys (5–7 years of age) were between 1 and 1.5 pmol/nmol free cholesterol, whereas in the PEC fractions, the levels were 3 to 5 times higher between 5 and 8 pmol/nmol free cholesterol. Eight monkeys were analyzed. The methodology used detects only free (unesterified) 7kCh and cholesterol. Because the samples were not saponified or subjected to any form of alkaline hydrolysis, the 7kCh levels might have been higher in areas containing oxidized CE-rich deposits. However, to our knowledge, esterified 7kCh is not toxic and has no known pharmacologic properties.

### Immunohistochemical Localization of 7kCh in Monkey Retina

To understand more about the formation of 7kCh in the retina and its potential for cytotoxicity, it was desirable to determine where (in what cell types and subcellular compartments) 7kCh resides. To obtain this information, we used a commercially available antibody that specifically recognizes 7kCh (see Materials and Methods). Frozen sections of monkey retinas were probed with anti-7kCh. 7-Ketocholesterol immunoreactivity was observed in the choriocapillaris and the retinal pigment epithelium (RPE)/Bruch's membrane regions (Figs. 2A, D). The outer wall (endothelial cell lining) of the inner retinal vasculature in the larger retinal vessels also demonstrated significant immunoreactivity (Fig. 2C). No background labeling was observed in the no-primary control (Fig. 2B). The contained nature of the immunoreactivity and the specific location suggest a possible association with oxidized lipoprotein deposits, which we have previously observed in similar locations by immunolocalization of apolipoprotein B.[33]

### Induction of VEGF by Oxidized LDLs and 7kCh in ARPE19 Cells

The location of 7kCh in the monkey retina (Fig. 2) suggested that it may be present in high enough local concentrations to affect the RPE and the choriocapillaris. Considering that oxLDL is known to contain high levels of 7kCh[4,5] and that 7kCh has been shown to induce VEGF in vascular smooth muscle cells,[15] we decided to investigate this effect in cultured RPE cells (ARPE19).

ARPE19 cells were treated with 50 $\mu$g/mL of the different LDLs (total lipid and protein weight) and were analyzed for cellular dehydrogenase activity and VEGF induction (Fig. 3). We used unoxidized native human LDL (control), copper oxidized LDL (Cu-oxLDL), and LDL, containing 7kCh (7kLDL). Cu-oxLDL had an oxidized lipid composition similar to that of

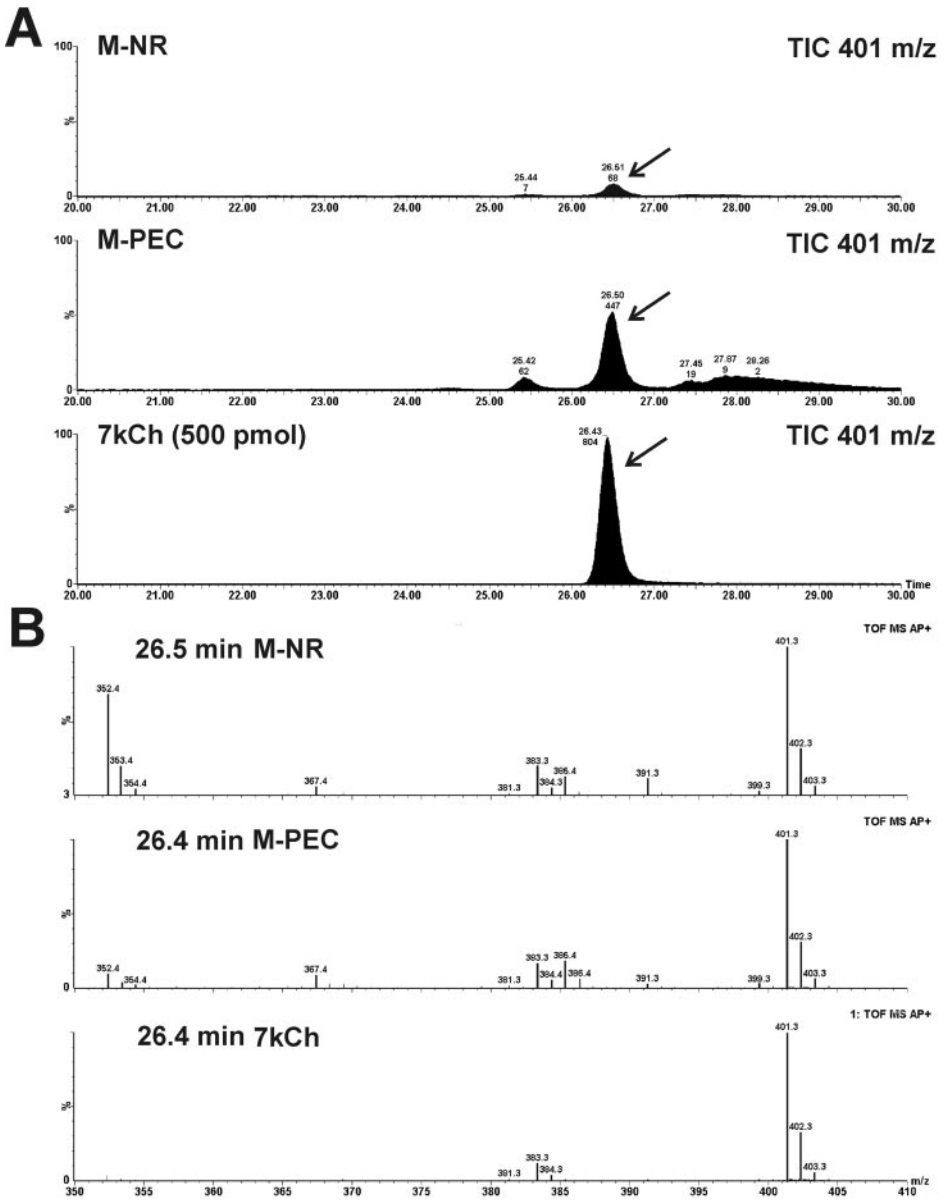


**FIGURE 1.** LC-MS of monkey retina extracts using APCi. (**A**) TIC for the 7kCh m/z 401 ion (M+H) found in extracts of monkey neural retina (M-NR) and pigment epithelium-choriocapillaris (M-PEC). (**B**) Mass spectra of the 26.4-minute peaks detected in (**A**). Retention times and mass spectra matched those of the 7kCh standard. Quantification was performed by area integration of the TIC peak for the specific ion.

oxLDL deposits found in atherosclerotic plaques.[4,5] The 7kLDL allowed the examination of the effects of 7kCh alone without all the other oxidized lipids found in oxLDL. VEGF induction was measured by qRT-PCR relative to GAPDH using commercially available TaqMan probes (Fig. 3A). Cellular dehydrogenase activity was measured to determine cell viability using the CCK-8 assay. After 24 hours, only 7kLDL demonstrated significant VEGF induction (3-fold; Fig. 3B), with a slight increase in the cellular dehydrogenase activity (Fig. 3A). After 48 hours of treatment, Cu-oxLDL showed a 2- to 3-fold VEGF induction and an increase in dehydrogenase activity (approximately 25%). 7kLDL showed a 7- to 10-fold VEGF induction (Fig. 3B), with a small reduction on cellular dehydrogenase activity (approximately 15%). The decrease in dehydrogenase activity observed with 7kLDL after 48 hours is indicative of cell death. This was also supported by visual examination of the cells (Fig. 3C). Increased cellular dehydrogenase activity was observed in these cells after treatment with different oxysterols (data not shown), which is independent of cell number because the cells are not dividing under these conditions. Most of the cellular dehydrogenase activity originated in the mitochondria, which suggested that the increased activity resulted from mitochondrial stress caused by the oxidized lipids.

These results suggested that 7kCh is the most likely component influencing VEGF induction. Thus, a similar experiment was performed (Fig. 4) using different amounts of 7kCh complexed with HPBCD. Lower concentrations of 7kCh also increased dehydrogenase activity significantly (approximately 25%; Fig. 4A; 4 and 8 $\mu$M), similar to the results obtained with LDLs (Fig. 3A). Maximum VEGF induction was observed using 12 $\mu$M 7kCh (Fig. 4B; 7- to 10-fold) in 24 hours. VEGF mRNA levels remained elevated at the higher concentrations (16 and 20 $\mu$M), though most cells were dead (Figs. 4A, 4C). At 48 hours, the 12 $\mu$M 7kCh concentration had essentially killed most of the cells, and VEGF mRNA levels did not increase after the initial induction at 8 $\mu$M (Fig. 4B).

To determine whether VEGF protein levels also increased during 7kCh treatment, conditioned media from the ARPE19 cells were analyzed by ELISA. After 24 hours there was little change in VEFG levels, but after 48 hours VEGF levels increased significantly after treatment with 8 and 12 $\mu$M VEGF (Table 1). At 8 $\mu$M 7kCh, cytotoxicity was minimal (Table 1;

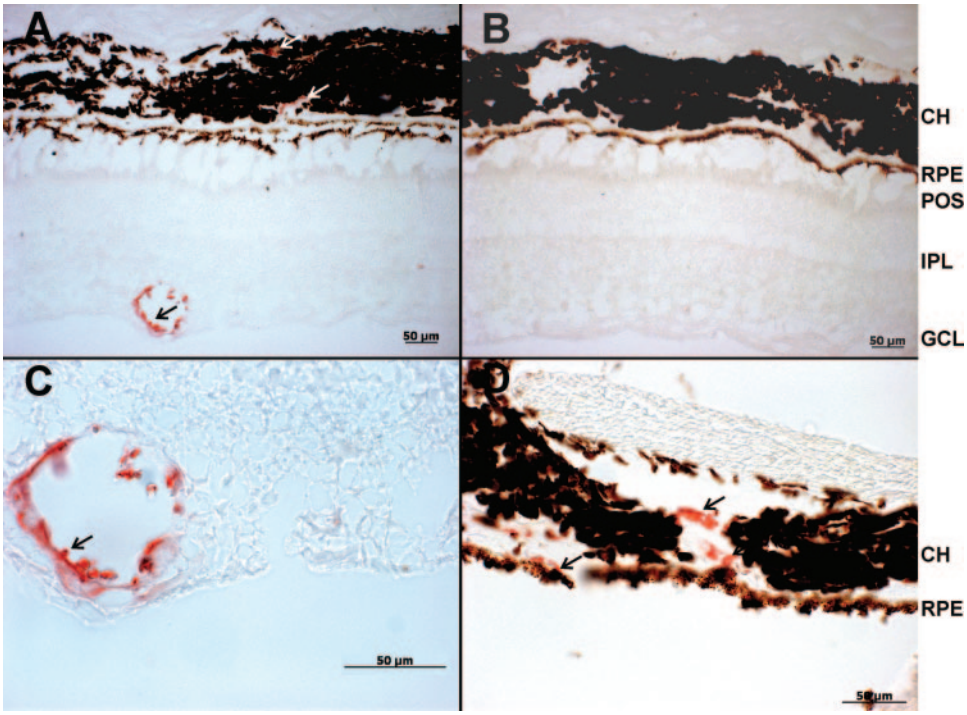


**FIGURE 2.** Immunohistochemical localization of 7kCh in monkey retina. Monkey frozen sections were treated with anti–7kCh antibody and the immunoreactivity was developed. Anti–7kCh immunoreactivity was observed mostly in the choroidal vessels and the RPE/Bruch's membrane region. (**A**) Low-magnification (20×) monkey retina. *Arrows*: Deposits. (**B**) No-primary control (20×). (**C**) Higher magnification (63×) neural retina vessel. (**D**) Higher magnification PEC region (40×). This localization is consistent with lipoprotein deposits.

Fig. 4). These results suggest that maximum VEGF mRNA induction seems to occur as mitochondrial stress reaches a threshold before the start of cell death. There seems to be a 24-hour lag in protein production and secretion.

## Induction of VEGF by Oxidized LDLs and 7kCh in HMVECs

Because the localization of 7kCh suggests that the vascular endothelial cells in the choriocapillaris seems to be the tissue most exposed to the 7kCh-containing deposits (Fig. 2), a vascular endothelial cell line (HMVEC) was also tested for comparison with the RPE-derived APRE19 cells.

HMVEC responded to the LDLs similarly to the ARPE19 cells in 24 hours (Fig. 5A, black) but were more susceptible to cytotoxicity from Cu-oxLDL and 7kLDL in the 48-hour time point (Fig. 5B, gray). Cells were treated with a lower dose (40 μg/mL) of LDLs. LDL increased dehydrogenase activity by approximately 40% but had no effect on VEGF induction. Cu-oxLDL increased dehydrogenase slightly in 24 hours (approximately 15%), but by 48 hours dehydrogenase activity was approximately 50% that of untreated controls. Cu-oxLDL in-

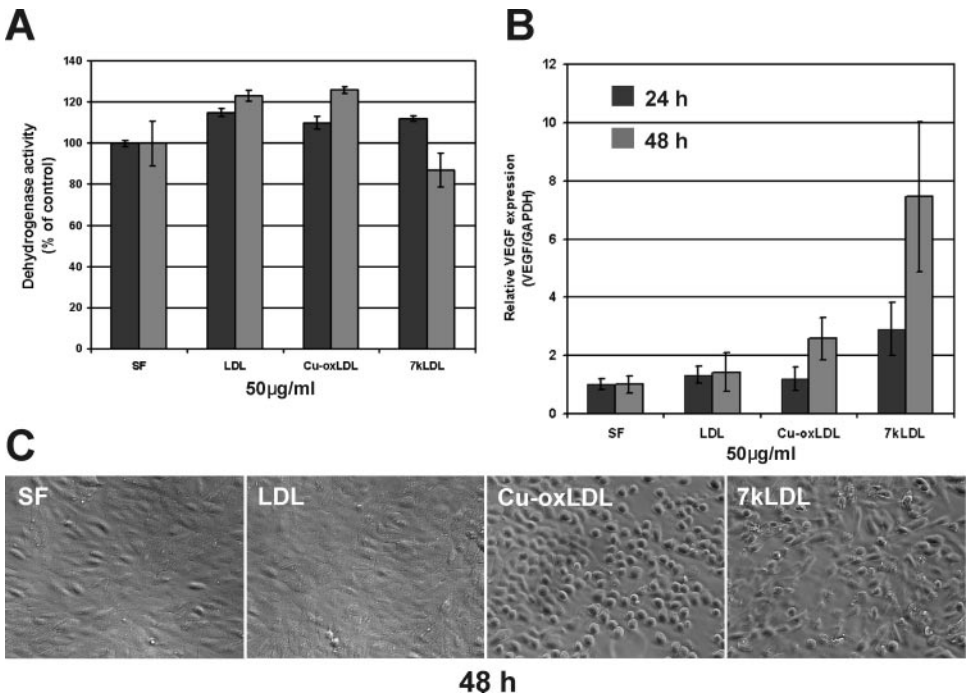


**FIGURE 3.** VEGF expression (mRNA) and cellular dehydrogenase activity in ARPE19 cells treated with 50 μg/mL LDL, oxLDL, and 7kLDL for 24 and 48 hours. (**A**) Relative dehydrogenase activity. (**B**) Relative VEGF mRNA expression measured by qRT-PCR. Error bars are the SD from four individual measurements. (**C**) Images of the cells 48 hours after each treatment.

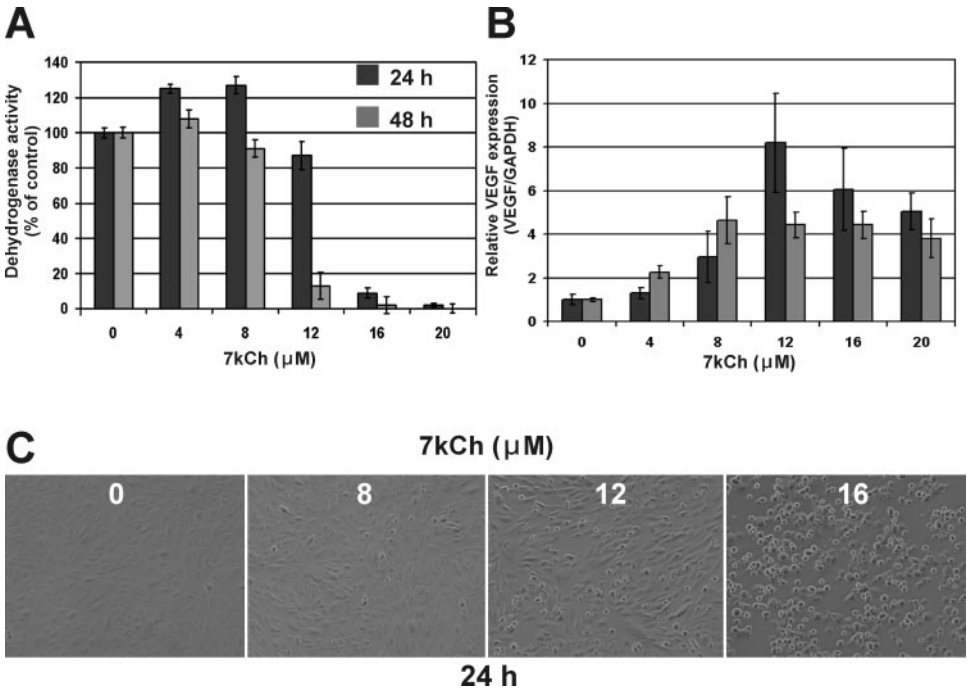


**FIGURE 4.** VEGF expression (mRNA) and cellular dehydrogenase activity in ARPE19 cells treated with 7kCh complexed with HPBCD. (**A**) Relative dehydrogenase activity. (**B**) Relative VEGF mRNA expression measured by qRT-PCR. Error bars are the SD from four individual measurements. (**C**) Images of the cells 24 hours after each treatment.

duced VEGF by approximately 2-fold over controls in 24 hours and by 3- to 4-fold in 48 hours. 7kLDL was similar to Cu-oxLDL in increasing the dehydrogenase activity in 24 hours (approximately 20%) and decreasing it (approximately 25%) by 48 hours. However, 7kLDL increased VEGF expression 4- to 5-fold in 24 hours and by 7- to 8-fold in 48 hours with less toxicity than Cu-oxLDL.

HMVEC also responded to 7kCh similarly to ARPE19 cells (Fig. 6). At 4 $\mu$M 7kCh, dehydrogenase activity was sharply increased at 24 and 48 hours (Fig. 6A) with a slight increase in VEGF induction (Fig. 6B). At 8 $\mu$M, there was a marked decrease in dehydrogenase activity at 24 and 48 hours (approximately 20% and 60% below controls, respectively), which correlated with a marked increase in VEGF induction (6- and 8-fold, respectively). At the higher concentrations (12–20 $\mu$M), there was marked cytotoxicity and cell death, and VEFG levels did not significantly change.

Although there were small differences in dose and tolerance to the oxidized lipids between the two cell types, they generally behaved similarly. 7kCh induced VEGF mRNA expression, and the highest levels of induction correlated with the beginning of cytotoxicity.

## Pathway of VEGF Induction by 7kCh

Oxidized LDL and 7kCh have been shown to induce VEGF in macrophages,[14] vascular smooth muscle cells,[15] and RPE, but

**TABLE 1.** Generation of VEGF Peptide in ARPE19-Conditioned Media 48 Hours after Treatment with Varying Amounts of 7kCh

| 7kCh ($\mu$M) | VEGF (pg/mL) | Cell Viability |
|---|---|---|
| 0 | 49 | 100 |
| 4 | 180 | 105 |
| 8 | 476 | 91 |
| 12 | 654 | 13 |
| 16 | 567 | 2 |
| 20 | 240 | 0 |

VEGF levels were measured with a human VEGF ELISA kit.

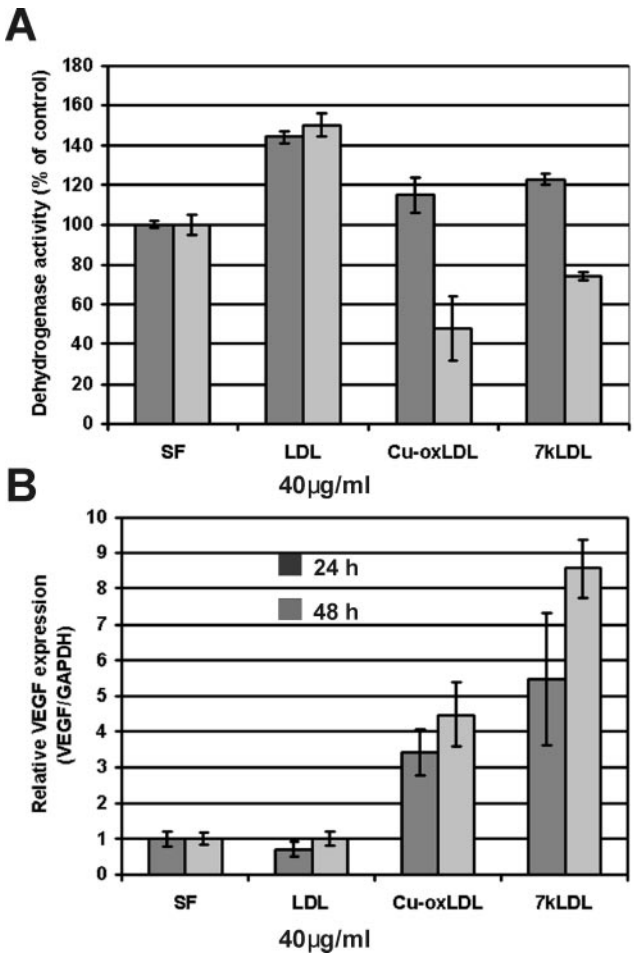


**FIGURE 5.** VEGF expression (mRNA) and cellular dehydrogenase activity in HMVECs treated with 40 $\mu$g/mL LDL, oxLDL, and 7kLDL for 24 and 48 hours. (**A**) Relative dehydrogenase activity. (**B**) Relative VEGF mRNA expression measured by qRT-PCR. Error bars are the SD from four individual measurements.

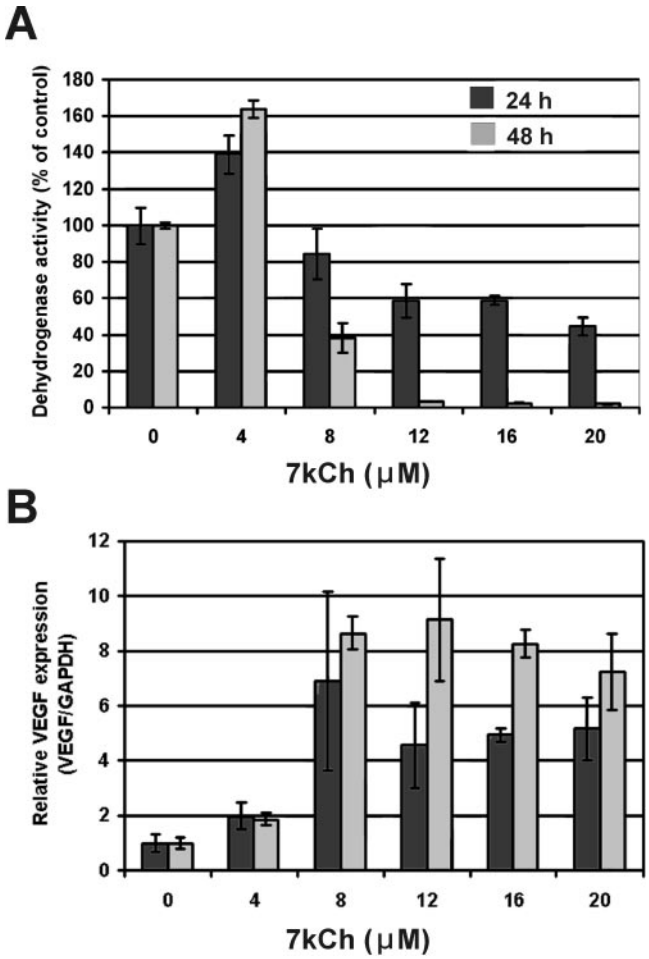


**FIGURE 6.** VEGF expression (mRNA) and cellular dehydrogenase activity in HMVECs treated with 7kCh complexed with HPBCD. (**A**) Relative dehydrogenase activity. (**B**) Relative VEGF mRNA expression measured by qRT-PCR. Error bars are the SD from four individual measurements.

the specific pathway for the 7kCh-mediated VEGF induction has not been elucidated. Results (Figs. 3–6) point to possible mitochondrial involvement because maximum VEGF induction correlated with the initiation of cytotoxicity (loss of dehydrogenase activity). This suggested that ROS and HIF-1$\alpha$ may be involved in mediating this induction.

HIF-1$\alpha$ is a transcription factor that interacts directly with the VEGF promoter.[34] We tested the involvement of this pathway in ARPE19 cells and used $CoCl_2$ as a positive control. $CoCl_2$ is known to increase HIF-1$\alpha$ levels by inhibiting its hydroxylation and preventing its ubiquitination and subsequent degradation.[11,18,35] HIF-1$\alpha$ is regulated at the protein level; therefore, we performed anti–HIF-1$\alpha$ immunoblots on ARPE19 cells treated with 7kCh and $CoCl_2$ (Fig. 7A). Results clearly demonstrated that 7kCh does not prevent HIF-1$\alpha$ degradation. Cellular dehydrogenase activity (cell viability) was measured at 100 and 200 $\mu$M $CoCl_2$ (Fig. 7B), and no appreciable loss of viability was observed up to 500 $\mu$M (data not shown). At these concentrations, $CoCl_2$ induced VEGF 3- to 4-fold over controls (Fig. 7C). At 15 $\mu$M 7kCh, approximately 50% loss of cell viability was observed (Fig. 7B).

With HIF-1$\alpha$ ruled out as a mediator, we examined the LXRs because they are known to mediate VEGF induction[21] and to interact with oxysterols, including 7kCh.[23] To determine their potential involvement, we used an LXR antagonist, cholesterol sulfate (ChS),[32] and siRNAs to both LXRs (Fig. 8).

ARPE19 cells were treated with 15 $\mu$M 7kCh with and without 20 $\mu$M ChS (Fig. 8A). Inductions of ABCA1 (control) and VEGF were measured by qRT-PCR. ABCA1 was used as a positive control because it is known to be almost exclusively regulated by LXRs.[36] ChS downregulated the expression of ABCA1 and VEGF (Fig. 8A) by 70% and 50%, respectively. Another LXR antagonist, 7kChS, downregulated ABCA1 and VEGF expression in a manner similar to that for ChS (data not shown). Neither ChS nor 7kChS is toxic to ARPE19 cells at the concentrations used.

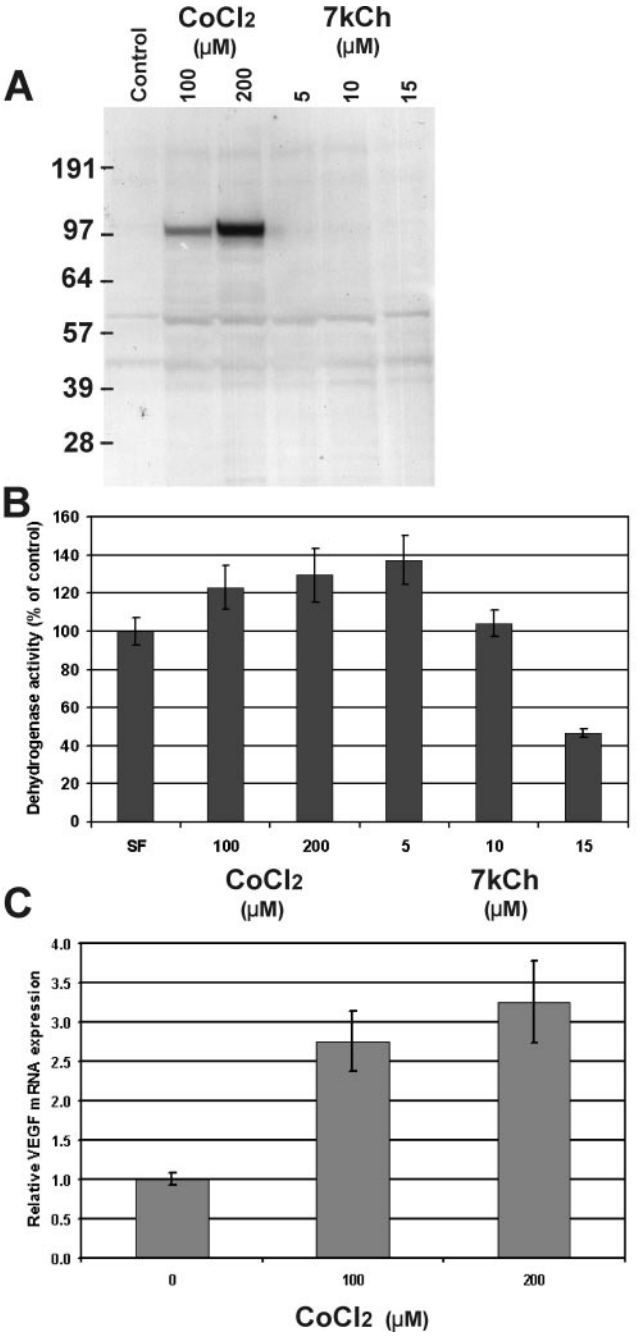


**FIGURE 7.** HIF-1$\alpha$ expression in APRE19 cells after $CoCl_2$ and 7kCh treatments. (**A**) Immunoblot of protein extract from ARPE19 cells before and after treatment with $CoCl_2$ and 7kCh. The blot was probed with anti–HIF-1$\alpha$ and developed. (**B**) Cellular dehydrogenase activity measured using the CCK-8 kit to determine cell viability.

To further demonstrate the involvement of LXRs, siRNAs were used to specifically suppress LXR$\alpha$ and LXR$\beta$ since both forms are expressed in retina and ARPE19 cells (data not shown). When the LXRs were suppressed individually, there was no significant difference in the ABCA1 and VEGF induction over controls (data not shown). However, when both LXRs were knocked down by a combination of siRNAs (Fig. 8B), ABCA1 and VEGF expression were similarly suppressed, suggesting that LXRs are involved in mediating VEGF induction by 7kCh. However, the lack of more significant attenuation by LXR siRNA suggests that other pathways may be involved in mediating this response.

NF-$\kappa$B mediates other HIF-independent pathways for the induction of VEGF and other cytokines.[20] To determine whether this pathway may be involved in the 7kCh-mediated VEGF induction, a known NF-$\kappa$B inhibitor, BAY 11-7082,[37] was used in combination with 15 $\mu$M 7kCh. We used IL-8 as a control because it is known to be regulated by NF-$\kappa$B[38] and to be induced by 7kCh.[39] IL-8 is also known to be induced in RPE cells.[40] BAY 11-7082 was used at 1 and 2 $\mu$M, and induction of IL-8 and VEGF was measured by qRT-PCR. Results are shown in Figure 9. Our data suggest that NF-$\kappa$B regulates 7kCh-mediated induction of IL-8 but not VEGF (Fig. 9A). In these experiments, cell viability remained between 60% and 80% (Fig. 9B).

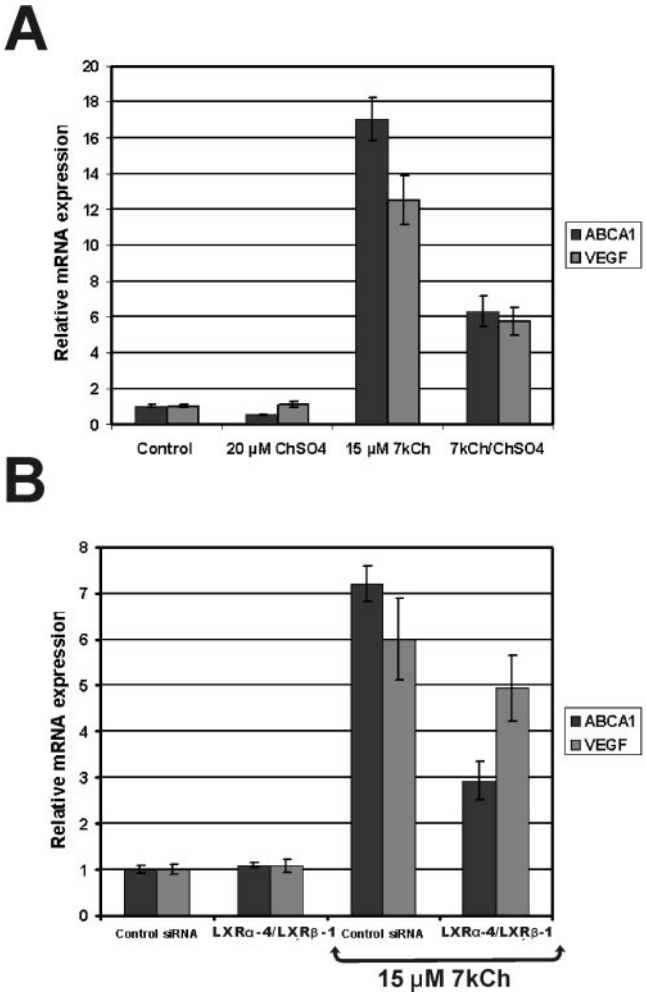


**FIGURE 8.** Effects of LXR antagonist and siRNA knockdown on 7kCh-induced VEGF expression in ARPE19 cells. (**A**) Cells were treated in serum-free media, with 15 $\mu$M 7kCh with or without 20 $\mu$M ChS, and were incubated for 24 hours. (**B**) Knockdown of LXRs using different siRNA combinations (1 LXR$\beta$), (4 LXR$\alpha$), and a negative control siRNA. The cells were given 15 $\mu$M 7kCh for VEGF induction. Levels of VEGF and ABCA1 (positive control) were measured by qRT-PCR.

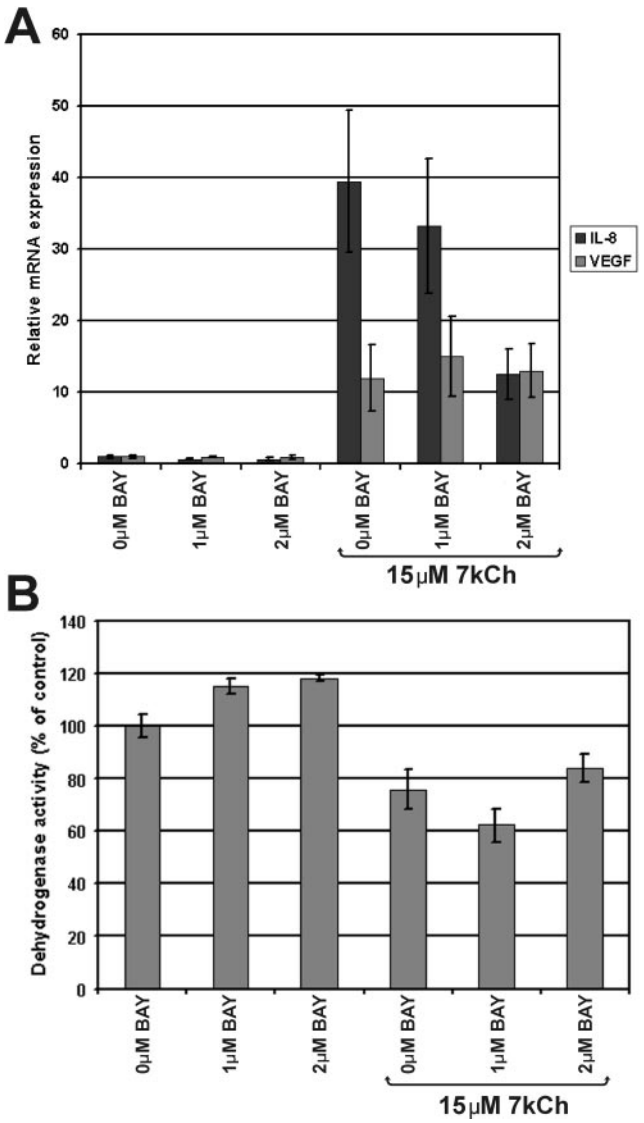


**FIGURE 9.** Effects of the NF-$\kappa$B inhibitor BAY 11-7082 on the 7kCh-mediated IL-8 and VEGF induction. (**A**) ARPE19 cells were treated with 0, 1, and 2 $\mu$M BAY with and without 15 $\mu$M 7kCh. (**B**) Cell viability measured using the CCK-8 dehydrogenase activity kit.

## DISCUSSION

7-Ketocholesterol is a well-studied cholesterol oxide known to have potent cytotoxic and pharmacologic properties.[1,2] Detection by LC-MS (Fig. 1) and location by immunohistochemistry (Fig. 2) in the primate retina raise several important questions concerning its origin and potential effects, especially in aging. The retina is known to accumulate lipids in the Bruch's membrane and the choriocapillaris as part of the aging process.[41,42] LDL, particularly when injected into rats, has been shown to form deposits in the choriocapillaris, Bruch's membrane, and RPE.[33,43] This suggests that most of the 7kCh found in the monkey retina (Fig. 2) is likely caused by oxidized lipoprotein deposits.

Oxidation of cholesterol to 7kCh is known to occur through two main mechanisms, the Fenton reaction[4] and photooxidation.[7] The Fenton reaction requires a transition metal catalyst;

iron and copper are particularly effective. CE-rich lipoproteins are particularly susceptible to Fenton oxidation,[4] and the cholesterol molecules in these esters can be efficiently oxidized to 7kCh.[4,5] Although the levels of copper and iron have not been measured in these deposits, atherosclerotic plaques are known to contain relatively high levels of these metals.[6] Photooxidation is another potential source of 7kCh in the retina, and fluorophores such as A2E may be able to serve as photosensitizers and oxidize cholesterol. A2E has also been reported to prevent cholesterol efflux from RPE cells.[44]

Levels of 7kCh in a healthy neural retina are low (approximately 1–4 pmol 7kCh/1 nmol Ch), but the amounts increase significantly in the PEC region (Fig. 1). Therefore, the focal localization of 7kCh in lipoprotein deposits could generate areas of very high concentrations that could have adverse affects on the cells that internalize or are in direct contact with these deposits. RPE cells abundantly express the LDL and the CD-36 receptors,[43] which can internalize most oxidized lipoproteins. Hence, the second part of our study focused on the potential effects of 7kCh on these cells.

It has been reported that oxLDL can induce VEGF in Raw-264 cells.[14] Given that overexpression of VEGF is one of the main problems in the formation of choroidal neovascularization (CNV), we examined the effects of oxLDL on VEGF expression in ARPE19 cells and HMVECs (Figs. 3, 6). In ARPE19 cells, we observed that Cu-oxLDL and 7kLDL had marked VEGF induction 48 hours after treatment (Fig. 3B). Cu-oxLDL induction was a modest 2- to 3-fold, whereas 7kLDL induction was a more vigorous 8- to 10-fold. Cellular dehydrogenase activity was increased (Fig. 3A) for all treatments in 24 hours but was slightly attenuated by 7kLDL in 48 hours. Images of cells at 48 hours after treatment suggested Cu-oxLDL and 7kLDL caused considerable cytotoxicity (Fig. 3C). These results suggested 7kCh may play an important role in VEGF induction.

VEGF expression was previously shown to be enhanced by 7kCh in vascular smooth muscle cells.[15] Thus, we tested 7kCh alone (in an HPBCD complex) to determine whether it could cause induction in these cells. The 7kCh treatment induced VEGF at 12 $\mu$M within 24 hours (Fig. 4B), and this correlated with signs of cytotoxicity (Figs. 4A, 4C). The same experiments were repeated with HMVECs, and similar results were obtained (Figs. 5, 6). HMVECs were slightly more responsive to Cu-oxLDL and 7kLDL than ARPE19 cells in VEGF induction and cytotoxicity (Fig. 5). Similar results were obtained with 7kCh alone; induction and cytotoxicity peaked around 8 $\mu$M (Fig. 6).

The mechanisms by which 7kCh induces VEGF have not been previously demonstrated. Understanding the pathway by which VEGF is induced in RPE and vascular endothelial cells may be important in understanding the pathogenesis of CNV. Therefore, we examined several factors that may modulate VEGF induction. 7kCh has been reported to induce mitochondrial ROS during apoptosis.[45] ROS formation is known to be involved in preventing HIF-1$\alpha$ degradation and VEGF induction through the HIF pathway.[16] However, when we examined HIF-1$\alpha$ protein expression in ARPE19 cells treated with 5, 10, and 15 $\mu$M 7kCh, no protein was found (Fig. 7A). Cobalt chloride was used as a positive control and caused a marked increase in HIF-1$\alpha$ protein levels (Fig. 7A) with little cytotoxicity (Fig. 7B). Cobalt chloride increased VEGF only 3- to 4-fold (Fig. 7C) compared with 8- to 10-fold for 7kCh (Figs. 4, 6, 7).

7kCh is known to interact directly with LXRs,[23] which have been previously reported to modulate VEGF expression in macrophages.[21] To determine whether LXRs may be involved in modulating 7kCh-mediated VEGF induction, we used two known LXR antagonists[32] and siRNA knockdowns (Fig. 8). ChS (Fig. 8) and 7kChS (data not shown) both attenuated ABCA1 and VEGF inductions by 7kCh (Fig. 8A). At 20 $\mu$M, ChS inhibited ABCA1 induction by 70% and VEGF induction by 50% (Fig. 8A), whereas 7kChS at 10 $\mu$M attenuated ABCA1 induction by 50% and VEGF induction by 40% (data not shown). When used individually, the siRNAs to LXR$\alpha$ and LXR$\beta$ had no effect on 7kCh-mediated VEGF induction (data not shown), but when used in combination, a measurable effect was detected (Fig. 8B). The LXR$\alpha$-1 and the LXR$\beta$-4 siRNA combination attenuated the ABCA1 response by 50% and the VEGF response by 20% to 30%. The fact that LXR siRNAs were unable to inhibit VEGF to the same extent as ABCA1 suggested that another pathway may contribute to VEGF induction.

Numerous other known pathways[10–13] can mediate VEGF induction, and we have not fully examined them all. NF-$\kappa$B is known to mediate the expression of many cytokines, including VEGF and IL-8. Inhibition of NF-$\kappa$B with BAY 11-7082 had no effect on 7kCh-mediated VEGF induction (Fig. 9). By contrast, IL-8, which was used as a positive control, was downregulated by approximately 75% with 2 $\mu$M BAY 11-7082 (Fig. 9A). Thus, the LXR pathway[21] seems to be the main induction pathway under these conditions.

The mechanism by which 7kCh induces VEGF in these cell types is not fully understood but seems to be HIF1 independent and to involve LXRs. These findings may have important implications in our understanding of the molecular mechanisms of CNV formation as it occurs in age-related diseases such as age-related macular degeneration.

## *References*


1. Lyons MA, Brown AJ. Molecules in focus: 7-ketocholesterol. *Int J Biochem Cell Biol.* 1999;31(3–4):369–375.
2. Jessup W, Wilson P, Gaus K, Kritharides L. Oxidized lipoproteins and macrophages. *Vacul Pharmacol.* 2002;38(4):239–248.
3. Hakamata H, Miyazaki A, Sakai M, Sakamoto YI, Horiuchi S. Cytotoxic effect of oxidized low density lipoprotein on macrophages. *J Atheroscler Thromb.* 1998; 5(2):66–75.
4. Dzeletovic S, Babiker A, Lund E, Diczfalusy U. Time course of oxysterol formation during in vitro oxidation of low density lipoprotein. *Chem Phys Lipids.* 1995;78(2):119–128.
5. Brown AJ, Dean RT, Jessup W. Free and esterified oxysterol: formation during copper-oxidation of low density lipoprotein and uptake by macrophages. *J Lipid Res.* 1996;37(2):320–335.
6. Stadler N, Lindner RA, Davies MJ. Direct detection and quantification of transition metal ions in human atherosclerotic plaques: evidence for the presence of elevated levels of iron and copper. *Arterioscler Thromb Vasc Biol.* 2004;24(5):949–954.
7. Girotti AW. Photosensitized oxidation of cholesterol in biological systems: reaction pathways, cytotoxic effects and defense mechanisms. *J Photochem Photobiol B.* 1992;13(2):105–118.
8. Girotti AW, Korytowski W. Cholesterol as a singlet oxygen detector in biological systems. *Methods Enzymol.* 2000;319:85–100.
9. Korytowski W, Bachowski GJ, Girotti AW. Photooxidation of cholesterol in homogeneous solution, isolated membranes, and cells: comparison of 5$\alpha$- and 6$\beta$-hydroperoxides as indicators of singlet oxygen intermediacy. *Photochem Photobiol.* 1992;56(1):1–8.
10. Ferrara N. Vascular endothelial growth factor: basic science and clinical progress. *Endocr Rev.* 2004;25(4):581–611.
11. Semenza GL. Hypoxia-inducible factor (HIF-1) pathway. *Sci STKE.* 2007(407):cm8.
12. Mizukami Y, Kohgo Y, Chung DC. Hypoxia inducible factor-1 independent pathways in tumor angiogenesis. *Clin Cancer Res.* 2007;13(19):5670–5674.
13. Pagés G, Pouysségur J. Transcriptional regulation of the vascular endothelial growth factor gene-a concert of activating factors. *Cardiovasc Res.* 2005;65(3):564–573.
14. Ramos MA, Kuzuya M, Esaki T, et al. Induction of macrophage VEGF in response to oxidized LDL and VEGF accumulation in human atherosclerotic lesion. *Arterioscler Thromb Vasc Biol.* 1998;18(7):1188–1196.
15. Dulakk J, Jozkowicz A, Dichtl W, et al. Vascular endothelial growth factor synthesis in vascular smooth muscle cells is enhanced by 7-ketocholesterol and lysophosphatidylcholine independently of

their effect on nitric oxide generation. *Atherosclerosis.* 2001; 159(2):325–332.
16. Taylor CT. Mitochondria and cellular oxygen sensing in the HIF pathway. *Biochem J.* 2008;409(1):19–26.
17. Xia C, Meng Q, Liu L-Z, Rojanasakul Y, Wang X-R, Jiang B-H. Reactive oxygen species regulate angiogenesis and tumor growth through vascular endothelial growth factor. *Cancer Res.* 2007; 67(22):10823–10830.
18. Ryan HE, Poloni M, McNulty W, et al. Hypoxia-inducible factor-1$\alpha$ is a positive factor in solid tumor growth. *Cancer Res.* 2000; 60(15):4010–4015.
19. Chandel NS, Trzyna WC, McClintock DS, Schumaker PT. Role of antioxidants and TNF-$\alpha$ gene transcription induced by hypoxia and endotoxin. *J Immunol.* 2000;165(2):1013–1021.
20. Kriakidis S, Andreakos E, Monaco C, Foxwell B, Feldmann M, Paleolog E. VEGF expression in human macrophages is NF-$\kappa$B-dependent: studies using adenoviruses expressing the endogenous NF-$\kappa$B inhibitor I$\kappa$B$\alpha$ and a kinase-defective form of the I$\kappa$B kinase 2. *J Cell Sci.* 2003;116(pt 4):665–674.
21. Walczak R, Joseph SB, Laffitte BA, Castrillo A, Pie L, Tontonoz P. Transcription of the vascular endothelial growth factor gene in macrophages is regulated by liver X receptors. *J Biol Chem.* 2004; 279(11):9905–9911.
22. Janowski BA, Willy PJ, Devi TR, Falck JR, Mangelsdorf DJ. An oxysterol signaling pathway mediated by the nuclear receptor LXR alpha. *Nature.* 1996;383(6602):728–731.
23. Janowski BA, Grogan MJ, Jones SA, et al. Structural requirements of ligands for the oxysterol liver X receptors LXR$\alpha$and LXR$\beta$. *Proc Natl Acad Sci U S A.* 1999;96:266–271.
24. Dusza JP, Joseph JP, Bernstein S. A fusion method for the preparation of steroid sulfates. *Steroids.* 1985;45(3–4):317–323.
25. Myoishi M, Hao H, Minamino T, et al. Increased endoplasmic reticulum stress in atherosclerotic plaques associated with acute coronary syndrome. *Circulation.* 2007;116:1226–1233.
26. Havel RJ, Eder HA, Bragdon JH. The distribution and chemical composition of ultracentrifugally separated lipoprotein in human serum. *J Clin Invest.* 1955;34(9):1345–1353.
27. Rodriguez IR, Alam S, Lee JW. Cytotoxicity of oxidized low density lipoprotein in cultured RPE cells is dependent on the formation of 7-ketocholesterol. *Invest Ophthamol Vis Sci.* 2004;45(8):2830–2837.
28. Bligh EG, Dyer WJ. A rapid method of total lipid extraction and purification. *Can J Biochem Physiol.* 1959;37(8):911–917.
29. Rodriguez IR. Rapid analysis of oxysterols by HPLC and UV spectroscopy. *BioTechniques.* 2004;36(6):952–958.
30. Kritharides L, Kus M, Brown AJ, Jessup W, Dean RT. Hydroxypropyl-$\beta$-cyclodextrin-mediated efflux of 7-ketocholesterol from macrophage foam cells. *J Biol Chem.* 1996;270(44):27450–27455.
31. Shao R, Guo X. Human microvascular endothelial cells immortalized with human telomerase catalytic protein: a model for the study of in vitro angiogenesis. *Biochem Biophys Res Commun.* 2004;321(4):788–794.
32. Song C, Hiipakka RA, Liao S. Auto-oxidized cholesterol sulfates are antagonistic ligands of liver X receptors: implications for the development and treatment of atherosclerosis. *Steroids.* 2001;66(6): 473–479.
33. Tserentsoodol N, Sztein J, Campos M, et al. Uptake of cholesterol by the retina occurs primarily via a low density lipoprotein receptor-mediated process. *Mol Vis.* 2006;12:1306–1318.
34. Liu Y, Cox SR, Morita T, Kourembanas S. Hypoxia regulates vascular endothelial growth factor gene expression in endothelial cells: identification of a 5′ enhancer. *Circ Res.* 1995;77(3):638–643.
35. Epstein AC, Gleadle JM, McNeill LA, et al. *C. elegans* EGL-9 and mammalian homologs define a family of dioxygenases that regulate HIF by prolyl hydroxylation. *Cell.* 2001;107(1):43–54.
36. Soumian S, Albrecht C, Davies AH, Gibbs RGJ. ABCA1 and atherosclerosis. *Vasc Med.* 2005;10(2):109–119.
37. Ohkita M, Takaoka M, Shiota Y, Nojiri R, Sugii M, Matsumura Y. A nuclear factor-$\kappa$B inhibitor BAY 11-7082 suppresses endothelin-1 production in cultured vacular endothelial cells. *Jpn J Pharmacol.* 2002;89:81–84.
38. Williams LM, Lali F, Willetts K, et al. Rac mediates TNF-induced cytokine production via modulation of NF-$\kappa$B. *Mol Immunol.* 2008;45(9):2446–2454.
39. Erridge C, Webb DJ, Spickett CM. 25-Hydroxycholesterol, 7$\beta$-hydroxycholesterol and 7-ketocholesterol upregulate interleukin-8 expression independently of Toll-like receptor 1, 2, 4 or 6 signaling in human macrophages. *Free Radic Res.* 2007;41(3):260–266.
40. Joffre C, Leclère L, Buteau B, et al. Oxysterols induced inflammation and oxidation in primary porcine retinal pigment epithelial cells. *Curr Eye Res.* 2007;32(3):271–280.
41. Curcio CA, Millican CL, Bailey T, Kruth HS. Accumulation of cholesterol with age in human Bruch's membrane. *Invest Ophthalmol Vis Sci.* 2001;42(1):265–274.
42. Ruberti JW, Curcio CA, Millican CL, Menco BP, Huang JD, Johnson M. Quick-freeze/deep-etch visualization of age-related lipid accumulation in Bruch's membrane. *Invest Ophthalmol Vis Sci.* 2003; 44(4):1753–1759.
43. Gordiyenko N, Campos M, Lee JW, Fariss RN, Sztein J, Rodriguez IR. RPE cells internalize low density lipoprotein (LDL) and oxidized LDL (oxLDL) in large quantities in vitro and in vivo. *Invest Ophthalmol Vis Sci.* 2004;45(8):2822–2829.
44. Lakkaraju A, Finnemann SC, Rodriguez-Boulan E. The lipofucin fluorophore A2E perturbs cholesterol metabolism in retinal pigment epithelial cells. *Proc Nat Acad Sci U S A.* 2007;104(26): 11026–11031.
45. Leonarduzzi G, Vizio B, Sottero B, et al. Early involvement of ROS overproduction in apoptosis induced by 7-ketocholesterol. *Antioxid Redox Signal.* 2006;8(3–4):375–380.